Inorganica Chimica Acta 520 (2021) 120299

Contents lists available at ScienceDirect

Inorganica Chimica Acta

journal homepage: www.elsevier.com/locate/ica

Research paper

Water-soluble Ag(I)-based coordination polymers obtained by anion-directed self-assembly of various AgX salts and a phosphabetaine derived from 1,3,5-triaza-7-phophaadamantane

Antal Udvardy [a,*], Csenge Tamara Szolnoki [a,b], Éva Kováts [c], Dávid Nyul [a,b], Gyula Tamás Gál [a], Gábor Papp [a], Ferenc Joó [a,d], Ágnes Kathó [a,*]

[a] Department of Physical Chemistry, University of Debrecen, P.O. Box 400, Debrecen H-4002, Hungary
[b] Doctoral School of Chemistry, University of Debrecen, P.O. Box 400, Debrecen H-4002, Hungary
[c] Institute for Solid State Physics and Optics, Wigner Research Centre for Physics, Konkoly Thege Miklós u. 29-33, H-1121 Budapest, Hungary
[d] MTA-DE Redox and Homogeneous Catalytic Reaction Mechanisms Research Group, P.O. Box 400, Debrecen H-4002, Hungary

ARTICLE INFO

Dedicated to Professor Maurizio Peruzzini in recognition of his numerous outstanding achievements in several branches of modern chemistry.

Keywords:
1,3,5-Triaza-7-phosphaadamantane
Coordination polymer
Ag-salts
Water-soluble
Diffusion NMR

ABSTRACT

A new, solvent-free method has been developed for the synthesis of 7-(2-carboxy-ethyl)-1,3,5-triaza-7-(phosphoniatricyclo)[3.3.1.1^{3,7}]decane (**L**). It is disclosed here that 1,3,5-triaza-7-phosphaadamantane (PTA) reacted cleanly with acrylic acid in a planetary ball mill resulting in 88% yield of the corresponding *P*-carboxy-ethyl derivative, in striking contrast to the complete failure of the synthesis of the same product from the same reactants in solution. The resulting phosphabetaine, **L** gave crystalline 1D coordination polymers with Ag^+-salts bearing PF_6^-, *p*-toluenesulfonate (tos) and trifluoromethanesulfonate (OTf) anions. According to single-crystal X-ray diffraction studies, the solid state structures of these coordination polymers were decisively influenced by the anion of the Ag^+-salt used for synthesis. In addition to single-crystal X-ray diffraction, the new Ag-based coordination polymers, namely $[Ag(\mu_3\text{-}\mathbf{L}\text{-}\kappa^3N{:}O{:}O')]_n(PF_6)_n$, (**1**), $[Ag(tos)(\mu_3\text{-}\mathbf{L}\text{-}\kappa^3N{:}N{:}O)]_n{\cdot}nH_2O$, (**2**), and $[Ag(OTf)(\mu_3\text{-}\mathbf{L}\text{-}\kappa^3N{:}O{:}O')]_n$, (**3**) were characterized also by elemental analysis, ^{1}H-, ^{13}C-, and ^{31}P NMR, as well as IR spectroscopies and with ESI mass spectrometry. Determination of the hydrodynamic diameter of the phosphabetaine ligand and its Ag^+-complexes by diffusion NMR measurements revealed, that upon dissolution in water these compounds did not retain their polymeric nature.

1. Introduction

Coordination polymers exhibit useful properties in several respects, such as, for example, catalysis, storage or separation of gases, luminescence, etc. [1–3]. The self-assembled, solid architectures can be modified relatively easily with the change of the metal ion or the complexing agents, or with the use of ancillary ligands. The resulting structures are influenced by several parameters, such as the temperature, pH, and the coordination ability of the solvent. In several cases, the anion of the applied metal salt also has an effect on the resulting structure [4–6] which is illustrated by the polymers obtained in the reaction of various Ag-salts and 1,3,5-triaza-7-phosphaadamantane (PTA; Scheme 1).

PTA is soluble in water and in polar organic solvents, and by virtue of its four donor atoms, it is capable of coordinating several (identical or different) metal ions [7–9]. The first PTA-containing water-soluble organometallic polymer was synthesized by Peruzzini, Romerosa and co-workers, in which Ru(II) and Ag(I) ions were held together by a *P*,*N*-coordinated ligand [10]. Other polymers were obtained by coordination of various metal ions, such as Au, Co, Zn to $[(Cp)Ru(PTA)_2Cl]$ [11–19]. PTA-based polymers, containing exclusively Ag(I)-ions, have also been described [20–29], several of which showed antitumor and antibacterial effects.

The first polymer in which PTA served as a tridentate bridging ligand between Ag(I) ions to form a 2D coordination network, was isolated from an aqueous solution containing PTA and $AgNO_3$ in equimolar amounts. In the polymer assembled from $[(Ag(\kappa OH_2)(\mu_3\text{-PTA-}\kappa^3P{:}N{:}N)]$

* Corresponding authors.
E-mail addresses: udvardya@unideb.hu (A. Udvardy), szolnoki.csenge@science.unideb.hu (C.T. Szolnoki), kovats.eva@wigner.mta.hu (É. Kováts), nyul.david@science.unideb.hu (D. Nyul), gal.tamas@science.unideb.hu (G.T. Gál), papp.gabor@science.unideb.hu (G. Papp), joo.ferenc@science.unideb.hu (F. Joó), katho.agnes@science.unideb.hu (Á. Kathó).

https://doi.org/10.1016/j.ica.2021.120299
Received 24 November 2020; Received in revised form 8 February 2021; Accepted 14 February 2021
Available online 20 February 2021

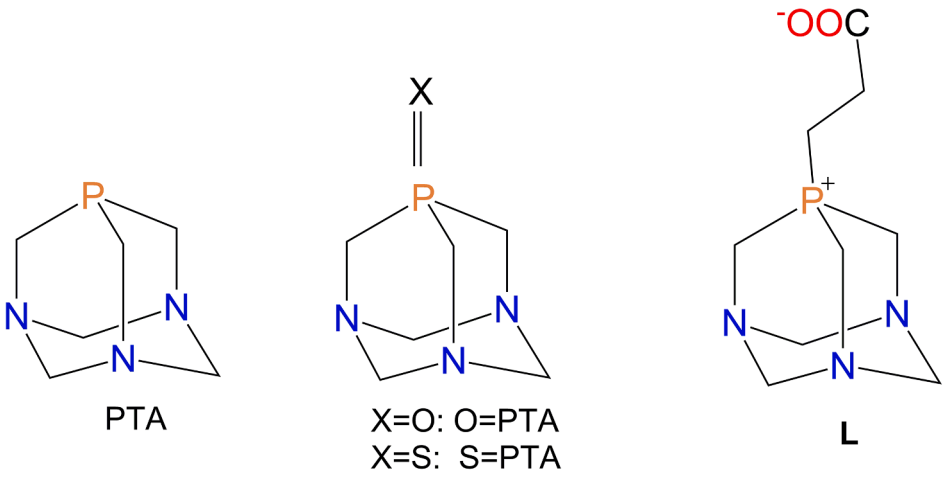

Scheme 1. PTA (1,3,5-triaza-7-phosphaadamantane), its oxide and sulphide and 7-(2-carboxy-ethyl)-1,3,5-triaza-7-(phosphoniatricyclo)[3.3.1.1^{3,7}]decane (**L**).

repeating units, each Ag^+ was coordinated by three PTA and one H_2O molecule in a distorted tetrahedral arrangement, while the anions were placed into the holes of the polymeric network [20]. However, when benzoic acid (or its derivatives) were added to a solution of PTA and $AgNO_3$ in a solvent mixture of MeOH:CH_2Cl_2:H_2O (5:5:0.5 mL), coordination polymers of diverse topologies were obtained, as a result of the effects of the carboxylate and other coordinating groups of the ancillary ligands [21]. Similar observations were made with the use of aliphatic dicarboxylic acids [22,24,26], substituted cyclohexanecarboxylic acids [22] and pyromellitic acid, too [28]. The influence of an ancillary reagent on the composition and structure of the products is conspicuously shown by the aqueous reaction of PTA with $Cu(NO_3)_2$, which –in the absence of any additive– yields $[Cu(PTA)_4](NO_3) \times 6H_2O$ but results in formation of the polymeric $[Cu(\mu\text{-}N_3)(\mu_2\text{-PTA:}\kappa^2P\text{:}N)]_n$ in presence of NaN_3 [30]. In fact, the latter compound was the first example of a homometallic 1D coordination polymer with PTA.

While the reaction of PTA with $AgNO_3$ yielded a polymer in which the nitrate anion did not coordinate to Ag^+ [20], in the polymers obtained with the use of Ag-nitrite, Ag-acetate, and Ag-trifluoroacetate the anions were bonded directly to the metal ion. In the ladder-type polymers $[Ag(\mu_2\text{-PTA:}\kappa^2P\text{:}N)(\mu_2\text{-}O_2N\text{:}\kappa^2O\text{:}O')]_n$ [27], $[(Ag(\mu_2\text{-PTA:}\kappa^2P\text{:}N)(\mu_2\text{-}O_2CCH_3\text{:}\kappa^2O\text{:}O')]_n{\cdot}2H_2O$, and $[(Ag(\mu_2\text{-PTA:}\kappa^2P\text{:}N)(\mu_2\text{-}O_2CCF_3\text{:}\kappa O\text{:}O')]_n{\cdot}nH_2O$ [29]. both PTA and the anions behaved as bidentate ligands.

The anions also influence the structure of the Ag(I)-based polymers obtained with PTA-oxide (O = PTA, Scheme 1). The product of complex formation between PTA-oxide and $AgNO_3$ was $[Ag(NO_3)(\mu_3\text{-}\{O = PTA\}\text{-}\kappa^3O\text{:}N\text{:}N)]_n$, however, the reaction of Ag_2SO_4 yielded $[Ag_2(\mu_2\text{-}SO_4)(\mu_5\text{-}\{O = PTA\})(H_2O)]_n$, in which three nitrogen atoms coordinate to one Ag^+, each, while the oxygen is bound to two Ag(I) ions [31]. The reaction of the same two Ag-salts with PTA-sulfide (S = PTA, Scheme 1), resulted in the formation of $[Ag(\mu_3\text{-}\{S = PTA\}\text{-}\kappa^3S\text{:}N\text{:}N)]_n(NO_3)_n{\cdot}nH_2O$ and $[Ag_4(\mu_2\text{-}SO_4)_2(\mu_4\text{-}\{S = PTA\})(\mu_5\text{-}\{S = PTA\})(H_2O)_2]_n \times 2nH_2O$ polymers [32–33]. In addition, in the coordination polymer $[Cu_6(\mu_3\text{-}I)_6(\mu_3\text{-}\{O = PTA\}\text{-}\kappa^3N\text{:}N\text{:}N)_2]_n$ (obtained in the reaction of Cu(I)-iodide and PTA = O), exclusive *N*-coordination of PTA-oxide was determined [34].

In the Morita-Baylis-Hillman type reaction of aldehydes with ethyl-acrylate, catalyzed by PTA, a P-substituted PTA derivative, 7-(2-carboxy-ethyl)-1,3,5-triaza-7-phosphonia-tricyclo[3.3.1.1^{3,7}]decane (**L**, Scheme 1) was isolated as a reaction intermediate [35,36].

In this paper, we report a new, mechanochemical synthesis of the above phosphabetaine, **L**. Furthermore, coordination chemical properties of **L** were investigated the first time. In aqueous solutions, reactions of **L** with three AgX salts (X= PF_6^-, $CF_3SO_3^-$, $CH_3C_6H_4SO_3^-$) resulted in formation of coordination polymers. The solid state structure of the polymers was determined by single crystal X-ray diffraction, while the molecular state of the polymers after dissolution in water was studied by diffusion NMR experiments. The results of these studies are also reported here.

2. Experimental part

2.1. Materials and methods

PTA was synthesized as described in the literature [37]. All other chemicals were commercial products of high purity and were used without further purification.

Elemental analyses were done on an Elementar Vario Micro (CHNS) equipment. High-resolution electrospray ionization mass spectra (HR ESI-MS) measurements were carried out on a Bruker maXis II MicroTOF-Q type Qq-TOF-MS instrument, controlled by Compass Data Analysis 4.4 software. Mass spectra were evaluated by the IsoPro 3.1 program. A Perkin Elmer Instruments Spectrum One FT-IR spectrometer equipped with a Universal ATR Sampling Accessory was used to record the IR spectra. Peak labelling: *w* (weak), *m* (medium), *s* (strong), *vs* (very strong).

NMR measurements were carried out with the use of BRUKER DRX 360 or Bruker Avance I 400 MHz spectrometers equipped with z-gradient BBI probe head. Chemical shifts were referenced to sodium 2,2-dimethyl-2-silapentane-5-sulfonate, DSS (^{1}H), (^{13}C) and to 85% H_3PO_4 (^{31}P). Spectra were evaluated with the use of the Bruker TopSpin 3.6.2 program. Multiplicities: *s* (singlet), *d* (doublet), *t* (triplet), *dt* (doublet of triplets), *h* (heptet), *m* (multiplet).

Diffusion NMR measurements [38–43] were carried out at 298 ± 0.2 K (Bruker BSCU 05 cooling unit) with the use of a stimulated spin echo pulse sequence together with a bipolar gradient (LEDBPGP2S) to minimize the effects of eddy currents. Diffusion of D_2O and the Ag(I)-based coordination polymers could be investigated with the same parameter set. Diffusion time $\Delta = 30$ ms, and gradient pulse length $\delta = 6$ ms were applied throughout. Gradient field strength (G) was varied in the 2–95% range in 32 quadratic steps. The maximum pulsed gradient strength was approximately 50 G cm^{-1}. Experimentally determined echo intensities were evaluated by the following equation:

$$I = I_{(0)} \times exp(-G^2\gamma^2\delta^2 D(\Delta - \delta/3))$$

where I and $I_{(0)}$ are the echo intensities at a given and at the initial gradient strength, respectively; G: pulsed gradient strength (T m^{-1}); γ: gyromagnetic ratio (MHz T^{-1}); Δ: diffusion time (s); D: diffusion coefficient (m^2 s^{-1}); δ: gradient pulse length (s). All experiments involved 32 measurement points and the series of resulting spectra were evaluated by the MestreNova © 8.1 software. The calibration constant of the

gradient field was left unchanged during the evaluation. The diffusion coefficient D_2O, determined with the use of the same constant, was equal to that known from the literature (1.902×10^{-9} m^2 s^{-1} [44]). From the experimentally determined diffusion constants (D) of the silver complexes, the hydrodynamic radii (R_D) of the diffusing species were obtained with the use of the Einstein–Stokes equation: $D_{exp} = k_BT(6\pi\eta R_D)^{-1}$ (k_B = Boltzmann constant, η = viscosity of the solution).

Single crystal X-ray diffraction measurements were made on a Bruker-Nonius MACH3 four-circle diffractometer [45] or on a SuperNova CCD diffractometer [46] with Mo Kα (λ = 0.71073) radiation in both cases. The structures were solved and refined with the use of SHELX [47,48] software packages, and managed by the OLEX^2 [49], and WINGX [50] crystallographic suites. The optimized structures of the molecules were analyzed with the use of PLATON [51], graphics were prepared with the Mercury [52] and OLEX^2 software.

The crystallographic data for all coordination polymers (including structure factors) were deposited in the Cambridge Crystallographic Data Centre (CCDC) with No 2046048, 2046052–2046053.

2.2. Synthesis of L and its Ag-based coordination polymers

2.2.1. 7-(2-carboxy-ethyl)-1,3,5-triaza-7-(phosphoniatricyclo)[3.3.1.1^{3,7}] decane (L)

A. In solution, ligand **L** was prepared by a modified literature procedure [35]. Under a well ventilated hood, in a 100 mL Schlenk flask, 500 mg (3.18 mmol) PTA was dissolved in 5 mL deoxygenated water, followed by the addition of 310 μL (3.4 mmol, ρ = 0.95 g/mL) methyl acrylate. To this reaction mixture, the minimum amount of acetone was added dropwise to obtain a homogeneous solution, which was then stirred at 70 °C for 7 h. The volatiles were removed under reduced pressure, the off-white residue was dissolved in 5 mL methanol, and filtered through a Hyflo Super Cel pad. The solvent was evaporated, the white residue was washed with 3 × 10 mL acetone followed by 2 × 10 mL diethyl ether. Yield: 752 mg (89%).

B. The mechanochemical procedure. Into a 12 mL RETSCH-type stainless steel jar were added 157 mg (1 mmol) PTA and 69 μL (1 mmol) acrylic acid together with 5 pieces of stainless steel milling balls (Ø 5 mm). The mixture was milled at 550 rpm for 2 h (in cycles of 2 min milling + 1 min cooling). The product was washed out from the jar with the minimum amount of water which was subsequently evaporated. The white residue was washed with 5 mL acetone followed by 5 mL diethyl ether. Yield 200 mg (88%).

The products of both procedures displayed spectroscopic characteristics identical to those published in the literature [35,36] (Fig. S1A, S1B).

Safety Warnings! Methyl acrylate is a colourless liquid with a burning smell. It is toxic and flammable, and its use requires a well-ventilated hood. Please, consult the MSDS sheet.

2.2.2. Reactions of 7-(2-carboxy-ethyl)-1,3,5-triaza-7-(phosphoniatricyclo)[3.3.1.1^{3,7}]decane (L) with AgX salts

To a solution of 100 mg (0.44 mmol) 7-(2-carboxy-ethyl)-1,3,5-triaza-7-(phosphoniatricyclo)[3.3.1.1^{3,7}]decane (**L**) in 4 mL water, was added with exclusion of light 1 mmol AgX (253 mg $AgPF_6$, or 257 mg $AgCF_3SO_3$ or 297 mg Ag-tosylate) dissolved in 3 mL water. 2-Propanol was layered on the top of the aqueous reaction mixtures which were then stored in the refrigerator. In about 2 weeks the products separated as colourless crystals which were isolated by filtration and washed with cold 2-propanol and finally dried.

$[Ag(\mu_3\text{-}\mathbf{L}\text{-}\kappa^3N{:}O{:}O')]_n(PF_6)_n$ (**1**)

Yield (based on **L**): 109 mg (51%)

^{1}H NMR (360 MHz, D_2O, 25 °C): δ 4.65 (d, J_{AB} = 13.5 Hz, 3H, *N*-C*H*^{A}*H*^{B}-N), 4.60 (d, $^2J_{PH}$ = 6.8 Hz, 6H, $^+$P-C*H*$_2$-N), 4.53 (d, J_{AB} = 13.2 Hz 3H, *N*-C*H*^{A}*H*^{B}-N), 2.59 (dt, $^2J_{PH}$ = 23.8, $^3J_{HH}$ = 6.5 Hz, 2H, P$^+$–C*H*$_2$-CH$_2$-COO$^-$), 2.35 (dt, $^3J_{PH}$ = 13.5, $^3J_{HH}$ = 6.5 Hz, 2H, P$^+$–CH$_2$-C*H*$_2$-COO$^-$) ppm (Fig. S2A).

^{13}C{^{1}H} NMR (90 MHz, , D_2O, 25 °C): δ 179.4 (d, $^3J_{PC}$ = 4 Hz, *C*OO$^-$), 71.6 (d, $^3J_{PC}$ = 9 Hz, N-*C*H$_2$-N), 49.0 (d, $^1J_{PC}$ = 38 Hz, $^+$P-*C*H$_2$-N), 29.0 (d, $^2J_{PC}$ = 7 Hz, P$^+$–CH$_2$-*C*H$_2$-COO$^-$), 18.6 (d, $^1J_{PC}$ = 36 Hz, P$^+$–*C*H$_2$-CH$_2$-COO$^-$) ppm (Fig. S2B).

^{31}P{^{1}H}NMR (145 MHz, D_2O, 25 °C): δ –37.5 (*s*), –145.0 (*h*) ppm (Fig. S2C).

Analysis: $C_9H_{16}AgF_6N_3O_2P_2$ (482.05): calcd. C 22.42, H 3.35, N 8.72; found C 22.42, H 3.50, N 8.78.

IR (ATR): ν/cm^{-1}: 505 (*m*), 556 (*vs*), 609 (*s*) 649 (*m*), 826 (*vs*), 944 (*vs*), 955 (*s*), 963 (*m*), 1109 (*m*), 1197 (*m*), 1238 (*s*), 1280 (*s*) 1291 (*s*), 1417 (*s*), 1538 (*s*), 1563 (*vs*) 1597 (*s*).

ESI-MS (positive ion mode; aqueous solution) most intense signals, *m/z*: [**L** + Na]$^+$, $C_9H_{16}N_3NaO_2P$, calcd. 252.0872, found 252.0878; and [2**L** + Na]$^+$, $C_{18}H_{32}N_6NaO_4P_2$, calcd. 481.1852, found 481.1854.

$[Ag(tos)(\mu_3\text{-}\mathbf{L}\text{-}\kappa^3N{:}N{:}O)]_n{\cdot}nH_2O$ (**2**)

Yield (based on **L**): 201 mg (90%)

^{1}H NMR (360 MHz, D_2O, 25 °C): δ 7.72 (d, $^3J_{HH}$ = 8.2 Hz, Ph, 2H), 7.40 (d, $^3J_{HH}$ = 8.2 Hz, Ph, 2H), 4.63 (d, J_{AB} = 13.6 Hz, 3H, *N*-C*H*^{A}*H*^{B}-N), 4.59 (d, $^2J_{PH}$ = 6.8 Hz, 6H, $^+$P-C*H*$_2$-N), 4.52 (d, J_{AB} = 13.2 Hz, 3H, *N*-C*H*^{A}*H*^{B}-N), 2.58 (dt, $^2J_{PH}$ = 23.7, $^3J_{HH}$ = 6.7 Hz, 2H, P$^+$–C*H*$_2$-CH$_2$-COO$^-$), 2.42 (s, 3H, CC*H*$_3$), 2.34 (dt, $^3J_{PH}$ = 13.5, $^3J_{HH}$ = 6.7 Hz, 2H, P$^+$–CH$_2$-C*H*$_2$-COO$^-$) ppm (Fig. S3A).

^{13}C{^{1}H} NMR (90 MHz, , D_2O, 25 °C): δ 179.4 (d, $^3J_{PC}$ = 4 Hz, *C*OO$^-$), 143.4 (s, Ph), 140.4 (s, Ph), 130.3 (s, Ph), 126.2 (s, Ph), 71.7 (d, $^3J_{PC}$ = 9 Hz, N-*C*H$_2$-N), 49.1 (d, $^1J_{PC}$ = 38 Hz, $^+$P-*C*H$_2$-N), 29.1 (d, $^2J_{PC}$ = 7 Hz, P$^+$–CH$_2$-*C*H$_2$-COO$^-$), 21.3 (s, –CH$_3$), 18.8 (d, $^1J_{PC}$ = 37 Hz, P$^+$–*C*H$_2$-CH$_2$-COO$^-$) ppm (Fig. S3B).

^{31}P{^{1}H}NMR (145 MHz, D_2O, 25 °C): δ –37.6 (*s*) ppm (Fig. S3C).

Analysis: $C_{16}H_{23}AgN_3O_5PS{\cdot}H_2O$ (526.29): calcd. C 36.51, H 4.79, N 7.98, S 6.09; found C 36.20, H 4.73, N 7.29, S 6.07.

IR (ATR): ν/cm^{-1}: 559 (*vs*), 569 (*vs*), 680 (*vs*), 705 (*w*), 755 (*s*), 779 (*s*), 813 (*s*), 911 (*m*), 944 (*vs*), 968 (*s*), 975 (*s*), 1009 (*vs*), 1031 (*vs*), 1118 (*vs*), 1174 (*vs*), 1204 (*vs*), 1302 (*m*), 1415 (*s*), 1557 (*s*), 1569 (*s*).

ESI-MS (positive ion mode; aqueous solution) most intense signals, *m/z*: [**L** + Na]$^+$, $C_9H_{16}N_3NaO_2P$, calcd. 252.0872, found 252.0880; [**L** + Ag]$^+$, $C_9H_{16}N_3AgO_2P$, calcd. 336.0026, found 336.0026; [2**L** + Na]$^+$, $C_{18}H_{32}N_6NaO_4P_2$, calcd. 481.1852, found 481.1854; and [2**L** + Ag]$^+$ $C_{18}H_{32}N_6AgO_4P_2$, calcd. 565.1005, found 565.1008.

$[Ag(OTf)(\mu_3\text{-}\mathbf{L}\text{-}\kappa^3N{:}O{:}O')]_n$ (**3**)

Yield (based on **L**): 106 mg (50%)

^{1}H NMR (360 MHz, D_2O, 25 °C): δ 4.65 (d, J_{AB} = 13.2 Hz, 3H, *N*-C*H*^{A}*H*^{B}-N), 4.60 (d, $^2J_{PH}$ = 6.8 Hz, 6H, $^+$P-C*H*$_2$-N), 4.52 (d, J_{AB} = 13.5 Hz, 3H, *N*-C*H*^{A}*H*^{B}-N), 2.59 (dt, $^2J_{PH}$ = 23.8, $^3J_{HH}$ = 6.5 Hz, 2H, P$^+$–C*H*$_2$-CH$_2$-COO$^-$), 2.35 (dt, $^3J_{PH}$ = 13.7, $^3J_{HH}$ = 6.7 Hz, 2H, P$^+$–CH$_2$-C*H*$_2$-COO$^-$) ppm (Fig. S4A).

^{13}C{^{1}H} NMR (90 MHz, , D_2O, 25 °C) δ 179.4 (d, $^3J_{PC}$ = 4 Hz, *C*OO$^-$), 122.3 (s, CF_3), 118.8 (s, CF_3), 71.9 (d, $^3J_{PC}$ = 9 Hz, N-*C*H$_2$-N), 49.4 (d, $^1J_{PC}$ = 37 Hz, $^+$P-*C*H$_2$-N), 29.2 (d, $^2J_{PC}$ = 7 Hz, P$^+$–CH$_2$-*C*H$_2$-COO$^-$), 18.8 (d, $^1J_{PC}$ = 37 Hz, P$^+$–*C*H$_2$-CH$_2$-COO$^-$) ppm (Fig. S4B).

^{31}P{^{1}H}NMR (145 MHz, D_2O, 25 °C) δ –37.6 (*s*) ppm (Fig. S4C).

Analysis: $C_{10}H_{16}AgF_3N_3O_5PS$ (486.15): calcd. C 24.71, H 3.32, N 8.64, S 6.60; found C 24.86, H 3.43, N 8.71, S 6.62

IR (ATR): ν/cm^{-1}: 516 (*vs*), 573 (*vs*), 604 (*vs*), 633 (*vs*), 749 (*vs*), 902 (*s*), 945 (*vs*), 973 (*vs*), 1008 (*vs*), 1028 (*vs*), 1152 (*vs*), 1169 (*vs*), 1225 (*vs*), 1256 (*vs*), 1290 (*vs*), 1411 (*s*) 1560 (*vs*), 1594 (*m*).

ESI-MS (positive ion mode; aqueous solution) most intense signals, *m/z*: [**L** + Ag]$^+$, $C_9H_{16}N_3AgO_2P$, calcd. 336.0026, found 336.0026; and [2**L** + Ag]$^+$, $C_{18}H_{32}N_6AgO_4P_2$, calcd. 565.1005, found 565.1008.

3. Results and discussion

3.1. Synthesis of 7-(2-carboxy-ethyl)-1,3,5-triaza-7-(phosphoniatricyclo)[3.3.1.1^{3,7}]decane (L)

The literature method of the synthesis of **L** involved stirring of PTA and six equivalents of ethyl acrylate at room temperature for 6 h in a

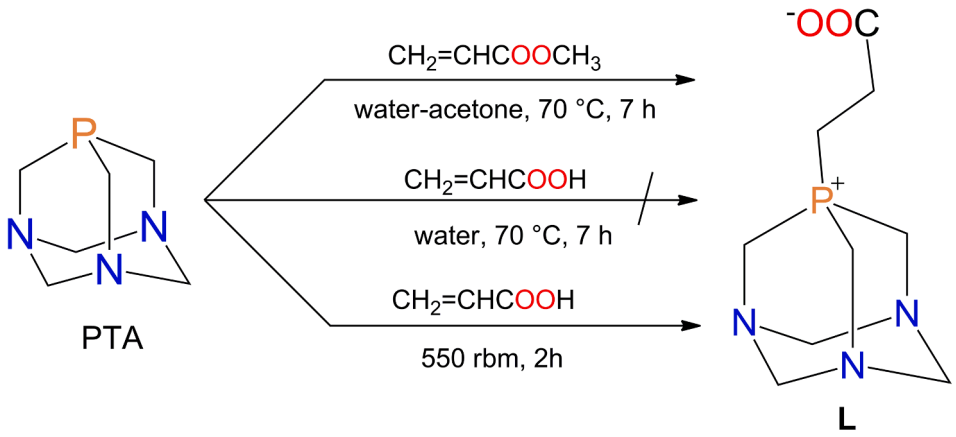

Scheme 2. Synthesis of 7-(2-carboxy-ethyl)-1,3,5-triaza-7-(phosphoniatricyclo)[3.3.1.1^{3,7}]decane (**L**).

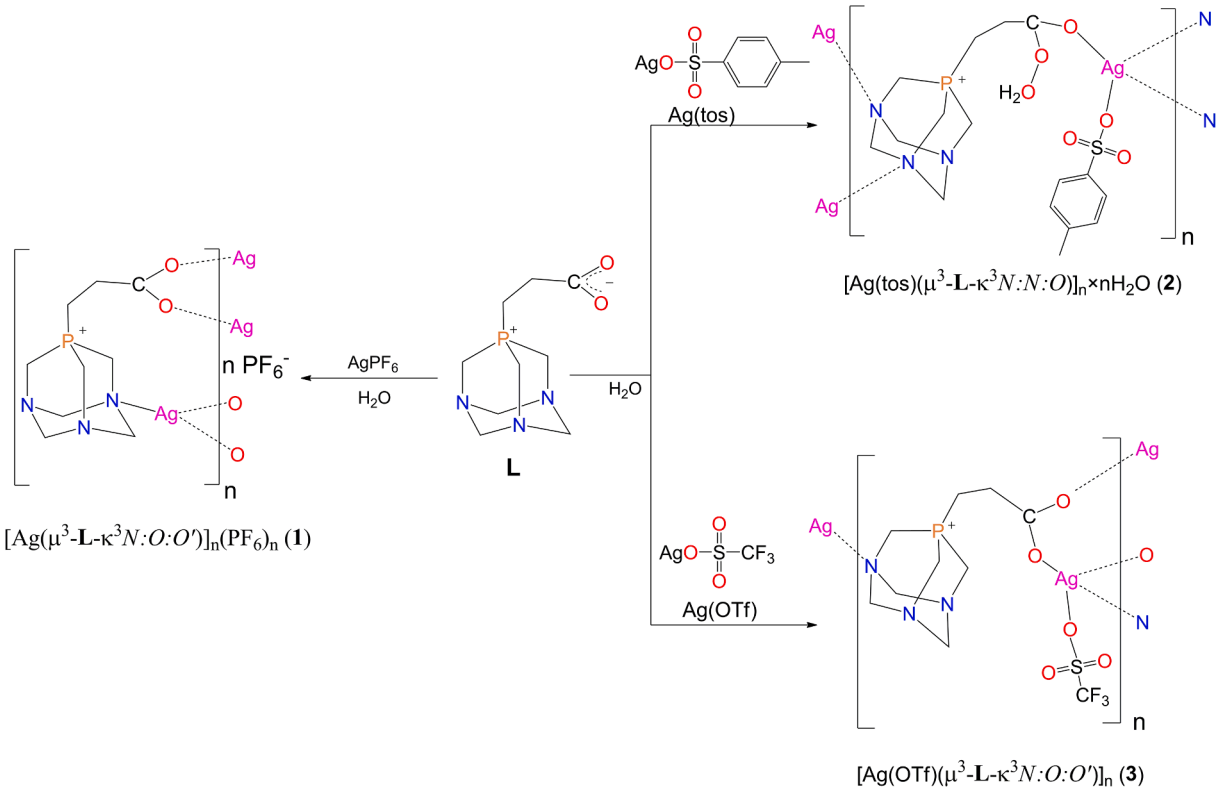

Fig. 1. Different coordination modes of **L** with various Ag-salts.

solvent mixture of THF-water (4:1, v/v) [35]. We have shown, that no excess of the acrylate is required since reaction of an equimolar mixture of PTA and methyl-acrylate in acetone–water at 70 °C results in the formation of the phosphabetaine **L** with 89% yield in 7 h (Scheme 2).

We have reported earlier, that reaction of PTA with unsaturated dicarboxylic acids in aqueous solution also led to the formation of phosphabetaines [53]. In contrast, in the reaction between acrylic *acid* and PTA, no P-substituted product was detected in aqueous solution even at 70 °C in 7 h. Conversely, when the same reaction was attempted under solvent-free conditions, after milling of PTA and acrylic acid in a planetary ball mill at 550 rpm for 2 h, **L** was isolated in 88% yield (Scheme 2). This is another excellent example, when mechanochemical procedures offer synthetic possibilities unavailable in solution synthesis or result in better yields and product qualities.

3.2. Synthesis and solid state structure of Ag-based coordination polymers of *L*

AgX salts (X=PF_6^-, $CF_3SO_3^-$, $CH_3C_6H_4SO_3^-$) were dissolved in water with exclusion of light, and added to the aqueous solutions of **L** (n_{Ag}:n_L = 2.27) also in the dark. The resulting solutions were layered with 2-propanol and were stored in a refrigerator. Colourless crystals were isolated (with 50–90% yield, depending on the AgX salt) which were not sensitive to oxygen or visible light. Microanalysis of the compounds showed that these crystals were 1:1 adducts of AgX and **L**. In the case of X = $CH_3C_6H_4SO_3^-$ (tosylate = tos) the product contained one molecule of water per one Ag^+, too.

The products were also obtained as single crystals and their structures were determined by X-ray diffraction. Fig. 1 shows the coordination modes determined by the anions.

Relevant crystal data and crystallographic measurement parameters

Table 1
Crystal data and structure refinement of the coordination polymers.

	1	2	3
Empirical formula	$[AgC_9H_{16}N_3O_2P]PF_6$	$[AgC_9H_{16}N_3O_2P](SO_3C_7H_7)(H_2O)$	$[AgC_9H_{16}N_3O_2P](CF_3SO_3)$
Formula weight	482.06	526.29	486.16
Crystal size [mm]	0.24 × 0.3 × 0.35	0.02 × 0.15 × 0.30	0.08 × 0.10 × 0.40
T [K]	293(2)	293(2)	293(2)
λ[Å]	0.71073	0.71073	0.71073
Crystal system	Orthorhombic	Monoclinic	Orthorhombic
Space group	$P2_12_12_1$	$P2_1/c$	$P2_12_12_1$
Crystal habit	colourless, block	colourless, plate	colourless, block
a [Å]	9.267(4)	17.6574(6)	9.3209(1)
b [Å]	11.818(2)	6.4618(2)	12.2181(2)
c [Å]	13.543(3)	17.1100(5)	13.9406(2)
α [°]	90	90	90
β [°]		92.250(2)	
γ [°]		90	
V[Å^3]	1483.2(8)	1950.72(11)	1587.61(4)
Z	4	4	4
Density (calc.) [g cm^{-3}]	2.159	1.792	2.034
Absorption coefficient (μ)[mm^{-1}]	1.652	1.262	1.563
F(000)	952	1072	968
2Θ range [°]	5.326 – 52.046	6.506 – 59.294	5.498 to 59.35
Index ranges	$0 \le h \le 11$, $-14 \le k \le 3$, $-16 \le l \le 16$	$-22 \le h \le 22$, $-8 \le k \le 8$, $-22 \le l \le 18$	$-12 \le h \le 12$, $-16 \le k \le 16$, $-17 \le l \le 19$
Total reflns.	3281	16,340	55,412
Unique reflns.	2904 [R_{int} = 0.0276]	4847 [R_{int} = 0.0357]	4324 [R_{int} = 0.0540]
Data/ restraints/ parameters	2904/0/208	4847/0/257	4324/0/217
Final R_1, wR_2(Obs. data)	0.0620, 0.1721	0.0374, 0.0732	0.0495, 0,1355
Final R_1, wR_2 (All. data)	0.0714, 0.2010	0.0553, 0.0827	0.0626, 0.1493
Goodness of fit (GOF) on F^2 (*S*)	1.153	1.064	1.012
$\Delta\rho_{max}/\Delta\rho_{min}$ [e. Å^{-3}]	1.79/–3.18	0.68/–0.75	1.52/–1.04
CCDC	2,046,048	2,046,052	2,046,053

are collected in Table 1.

The polymer formed in the reaction of **L** and $AgPF_6$, $[(Ag(\mu_3\text{-}\mathbf{L}\text{-}\kappa^3\textit{N:O:O'})]_n(PF_6)_n$ (**1**), crystallizes in the orthorhombic $P2_12_12_1$ space group. In addition to the N,O,O'-coordinated Ag(I), there is a zwitterionic **L** and a discrete PF_6-ion in the asymmetric unit (Fig. S5A). Although crystallization was performed from water, neither Ag-coordinated H_2O nor water of crystallinity were found in the crystal (Fig. 1).

The bond lengths and angles of the Ag-coordinated phosphabetaine agree within the limits of accuracy with the same parameters in the free **L** described before [36]. A notable exception is the *P*1-O11 distance (2.639(10) Å) which is shorter in **1** than in **L** (2.661 Å). In **1**, each Ag(I) atom is surrounded by three phosphabetaine molecules (Fig. 1, Fig. S5B). Two of these phosphabetaines coordinate to the Ag(I) atom with one of their carboxylate oxygens, while the third **L** binds to the same Ag(I) with one nitrogen atom of the phosphadamantane moiety, altogether resulting in a slightly distorted trigonal, Y-shape coordination geometry (Fig. 1). There are 17 structures reported in the literature in which PTA is coordinated with its nitrogen to an Ag(I)-ion. In those complexes, the characteristic Ag-$N_{(PTA)}$ distance is in the range of a 2.302–2.541 Å [54], i.e. the Ag-$N_{(PTA)}$ distance in **1** (2.232(11)Å) is shorter.

The bridging coordination of the **L** ligands to two silver ions results in formation of chain polymers (Fig. 2, Fig. S5C). The packing diagram (Fig. 1) shows that with the involvement of two Ag^+ ions and two **L** ligands, 12-membered macrocycles are formed, in which the Ag(1)…Ag(1) distance is 5.085 Å, indicating no interaction between the metal ions.

The crystal lattice is held together by weak C—H…O and C—H…F hydrogen bonds (Figs. S5D-S5F) and the PF_6-ions occupy the voids between the polymer backbones. The bond length data indicating weak interactions are contained in Table S1.

Formation of the coordination polymer, $[Ag(tos)(\mu_3\text{-}\mathbf{L}\text{-}\kappa^3\textit{N:N:O})]_n{\cdot}nH_2O$ (**2**), obtained in the aqueous reaction of Ag(tos) and **L**, is assisted by the O-donor atom of the anion (Fig. 3). The compound crystallizes in the centrosymmetric monoclinic $P2_1/c$ space group. In the asymmetric unit, in addition to the Ag(I)-ion, **L** and the tosylate anion, a water molecule is found, too (Z = 4) (Fig. S6A).

In contrast to the $\{[Ag_3(tos)_3(hmt)_3(H_2O)] \times 3H_2O\}_n$ polymer [55] obtained in the reaction of Ag(tos) and hexamethylenetetramine (hmt, urotropine), in **2,** nitrogen donor atoms of only two (and not all three) **L** phosphabetaines are coordinated to Ag(I) (Fig. 3). The Ag1–N1$^{(i)}$ bond lengths (2.363(2) Å) agree well with the average values determined for

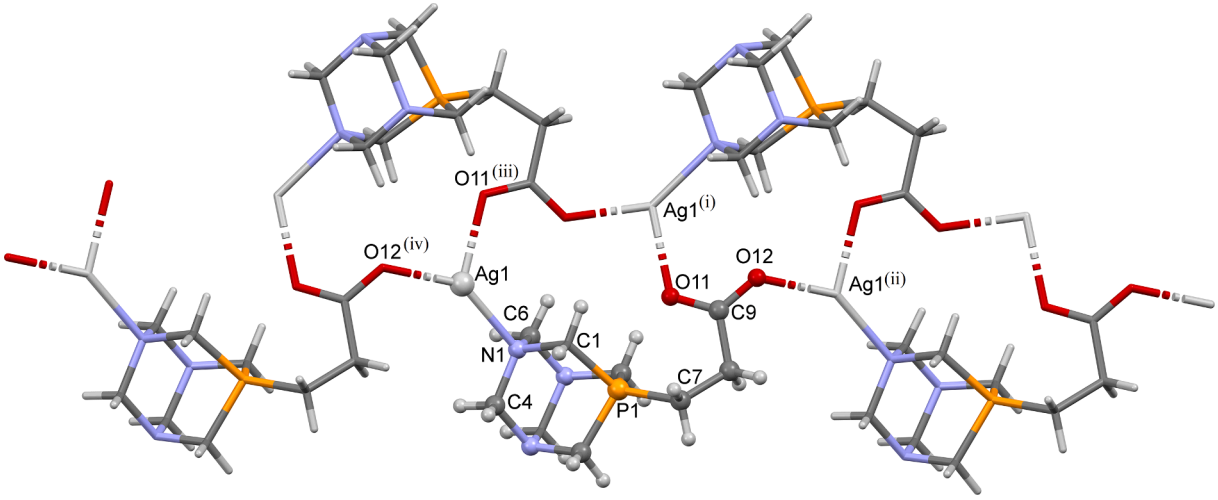

Fig. 2. Coordination environment of Ag(I) in $[(Ag(\mu_3\text{-}\mathbf{L}\text{-}\kappa^3\textit{N:O:O'})]_n(PF_6)_n$, (**1**). The asymmetric unit of **1** is given in ball and sticks, and the symmetry-generated part of the polymer is given in capped sticks representation. PF_6-ions are omitted for clarity. Selected bond lengths (Å) and angles (°) Ag1–N1 = 2.232(11), Ag1–O11$^{(iii)}$ = 2.291(9), Ag1–O12$^{(iv)}$ = 2.210(10), O11–Ag1$^{(i)}$ = 2.291(9), O12–Ag1$^{(ii)}$ = 2.210(10), O11–*P*1 = 2.639(10), C1–N1–Ag1 = 104.5(7), C4–N1–Ag1 = 115.4(8), C6–N1–Ag1 = 106.7(8), C9–O11–Ag11 = 117.8(8), C9–O12–Ag12 = 122.1(8), N1–Ag1–O11$^{(iii)}$ = 120.8(3)°, O12$^{(iv)}$–Ag1–N1 = 144.3(4) and O11$^{(iii)}$–Ag1–O12$^{(iv)}$ = 94.8(3)°; [Symmetry codes: (i) 1/2 + x, 3/2–y, 2–z; (ii) 1 + x, +y, +z; (iii) –1/2 + x, 3/2–y, 2–z; (iv) –1 + x, +y, +z].

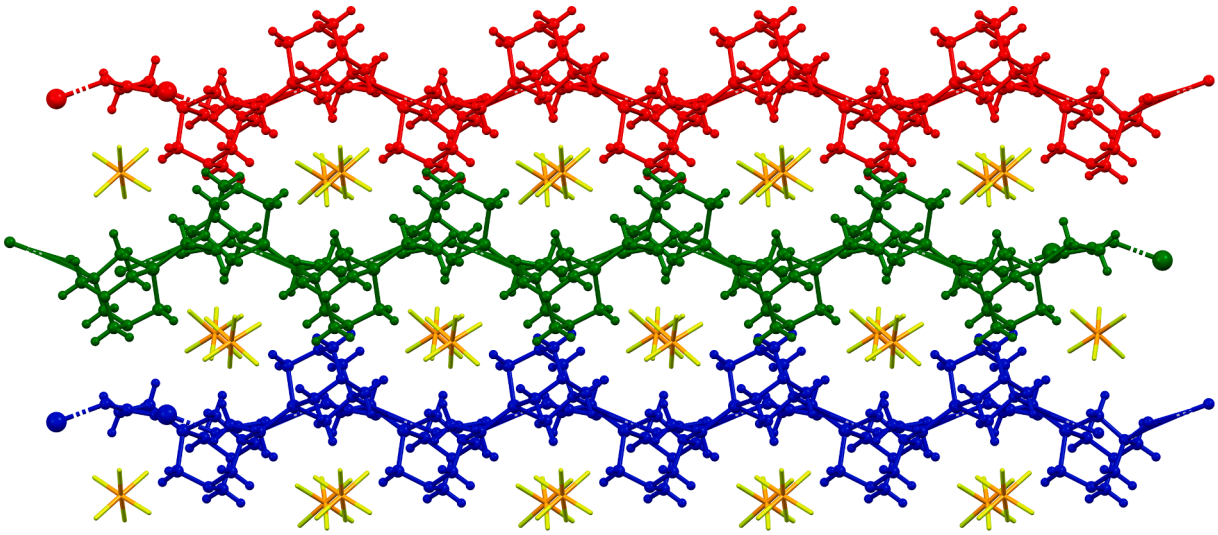

Fig. 3. Ag-based polymer chains in the lattice of $[(Ag(\mu_3\text{-}\mathbf{L}\text{-}\kappa^3 N{:}O{:}O')]_n(PF_6)_n$, (**1**). (Each chain is drawn in a different color).

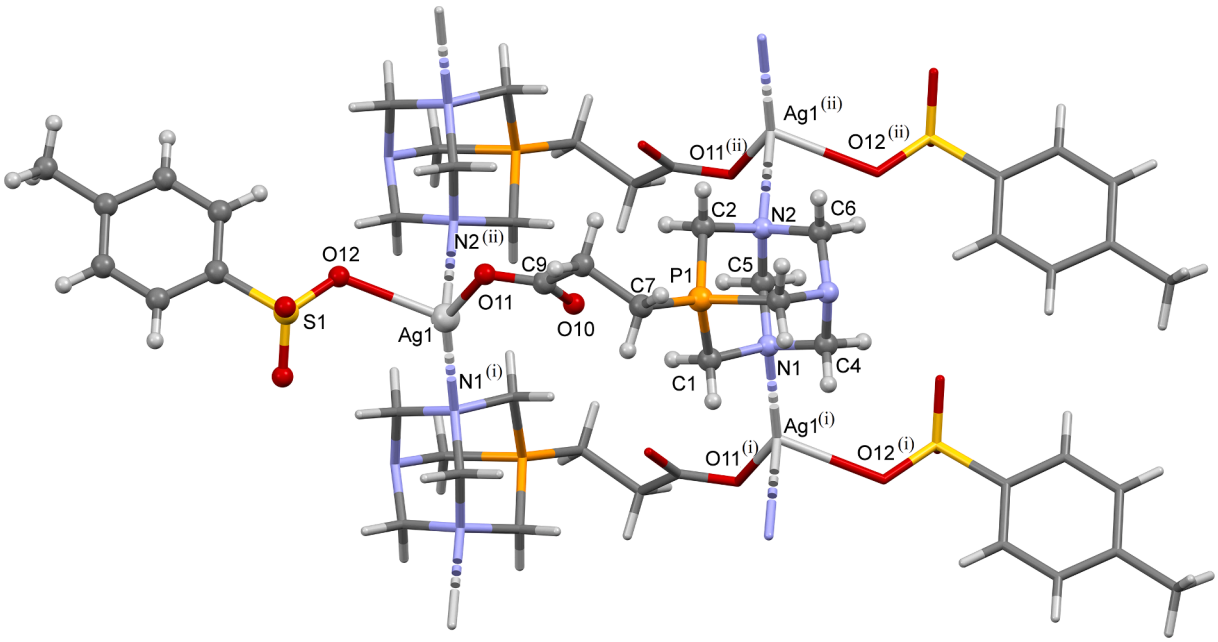

Fig. 4. Coordination environment of Ag(I) in $[Ag(tos)(\mu_3\text{-}\mathbf{L}\text{-}\kappa^3 N{:}N{:}O)]_n{\cdot}nH_2O$, **2.** The asymmetric unit of **2** is given in ball and sticks, and the symmetry-generated part of the polymer is given in capped sticks representation. Water molecules are omitted for clarity. Selected bond length (Å) and angles (°): Ag1–O11 = 2.284(2), Ag1–N1$^{(i)}$ = 2.363(2), Ag1–O12 = 2.417(2), Ag1–N2$^{(ii)}$ = 2.577(2), N1–Ag$^{(i)}$ = 2.363(2), N2–Ag$^{(ii)}$ = 2.363(2), *P*1–C7 = 1.796(3), O11–Ag1–N1$^{(i)}$ = 140.56(8), O11–Ag1–O12 = 95.78(9), O11–Ag1–N2 = 99.36(8), N1$^{(i)}$–Ag1–O12 = 115.64(9), N1$^{(i)}$–Ag1–N2$^{(ii)}$ = 108.18(8), O12–Ag1–N2$^{(ii)}$ = 81.05(7), C9–O11–Ag1 = 106.12 (19), C5–N1–Ag1$^{(i)}$ = 119.37(17), C1–N1–Ag1$^{(i)}$ = 101.40(16), C4–N1–Ag1$^{(i)}$ = 105.67(16), S1–O12–Ag1 = 124.42(14), *C*2–N2–Ag1$^{(ii)}$ = 111.76(16), C5–N2–Ag1$^{(ii)}$ = 103.42(15), C6–N2–Ag1$^{(ii)}$ = 109.17(16); [Symmetry codes: (i) 1–x,–y,1–z; (ii) 1–x,1–y,1–z].

Ag-PTA complexes (2.302–2.541 Å [54]). However, the Ag1–N2$^{(ii)}$ distance (2.577(2) Å) is larger than the longest Ag-N distance determined for an Ag-PTA complex, namely (2.541 Å) found in $[Ag_2(\mu_4\text{-PTA})(\mu_4\text{-mal})]_n$ (mal: malonato) [26].

In **2**, the Ag(I)-ion is found in a distorted tetrahedral (AgN_2O_2) coordination geometry. Two ligands are *N*-bonded, while the tosylate anion and the third **L** coordinate through one of their oxygen donor atoms, (Fig. 3, Fig. S6A-S6B). There is no interaction between the metal ion and the other carboxylate oxygen atom of **L** (Ag1–O10 = 2.859(2) Å).

With the participation of one silver ion, two phosphabetaine ligands and two tosylate anions, 16-membered macrocycles are formed, which overlap and form a tube-like array (Fig.s S6B-S6C). The structure is held together by strong hydrogen bonds between the neighbouring stacked macrocycles. Network of hydrogen-bonds are formed with participation of carboxylate oxygen atoms (O10 and O11) of coordinated **L**, and water molecules of the crystal structure. The outcome is a 1D polymer network (Fig. 4, Figs. S6D-S6F).

There are also weak C—H…O interactions between the polymer chains (Table S2). Surprisingly, no π- π stacking interactions can be observed between the aromatic units of tosylate anion.

In the coordination polymer $[Ag(OTf)(\mu_3\text{-}\mathbf{L}\text{-}\kappa^3 N{:}O{:}O')]_n$ **(3)** (for unit cell see Fig. S7A-S7B), a different coordination mode can be observed than in **2**, although this polymer contains a similar sulfonate-bearing anion, triflate (OTf). **3** crystallizes in the common orthorhombic $P2_12_12_1$ space group. The molecular structures of the free and

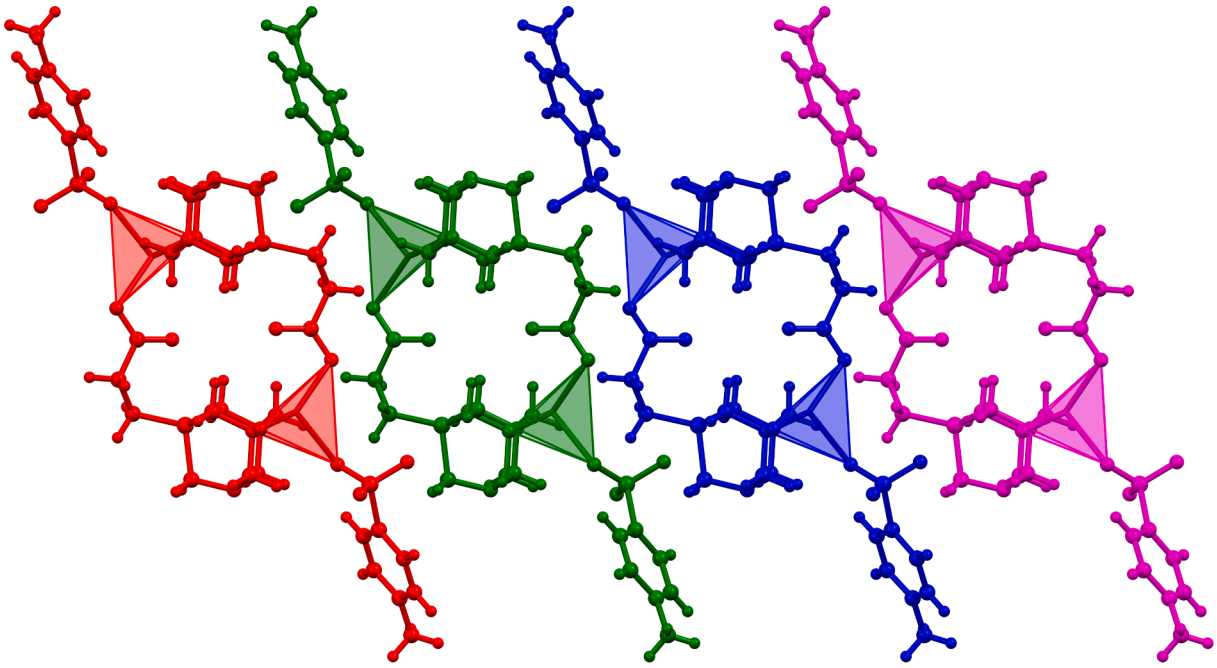

Fig. 5. Tube-like arrays in the lattice of [Ag(tos)(μ_3-**L**-κ^3*N:N:O*)]$_n$·nH_2O, **2.** (Each tube with polyhedrons of silver atoms is drawn in a different color.)

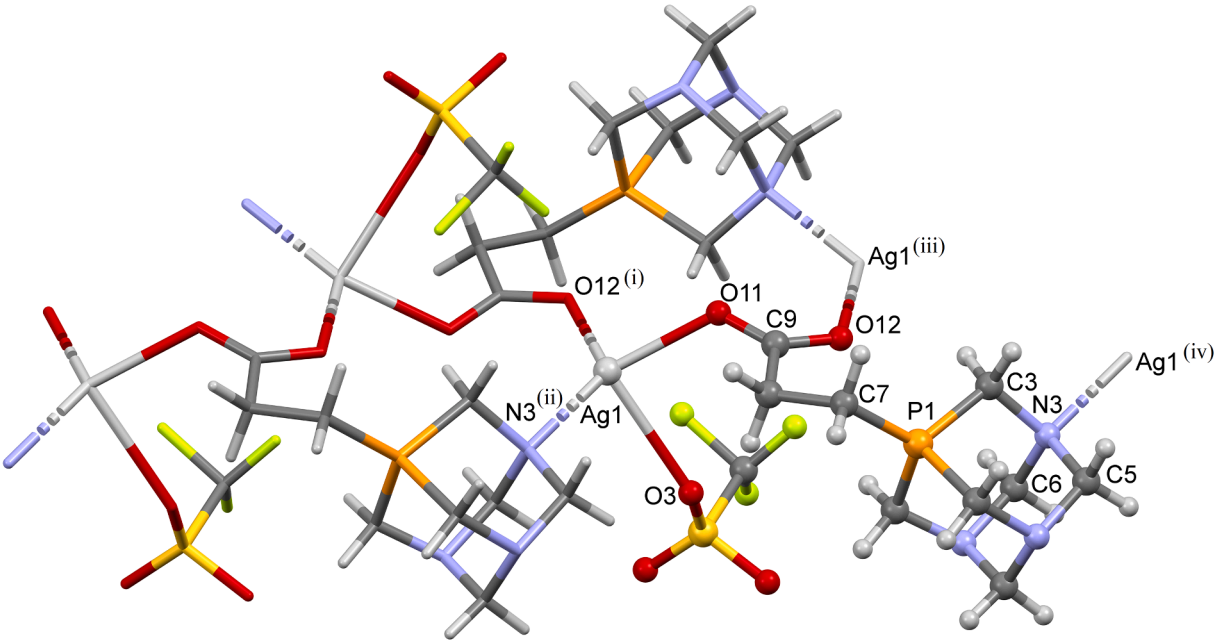

Fig. 6. Coordination environment of Ag(I) in [Ag(OTf)(μ_3-**L**-κ^3*N:O:O'*)]$_n$, **3**. The asymmetric unit of **3** is given in ball and sticks, and the symmetry-generated part of the polymer is given in capped sticks representation. Selected bond lengths (Å) and angles (°): Ag1–O11 = 2.260(5), Ag1–O12$^{(i)}$ = 2.290(5), Ag1–N3$^{(ii)}$ = 2.288(6), *P*1–C7 = 1.801(7), O12–Ag1$^{(iii)}$ = 2.290(5), N3–Ag1$^{(iv)}$ = 2.288(6), Ag1–O3 = 2.692(9), O11–Ag1–O12$^{(i)}$ = 96.3(2), O11–Ag1–N3$^{(ii)}$ = 139.6(2), O12$^{(i)}$–Ag1–N3$^{(ii)}$ = 122.0(2), C9–O11–Ag1 = 123.8(5), C9–O12–Ag1$^{(iii)}$ = 119.1(5), C3–N3–Ag1$^{(iv)}$ = 105.0(4), C6–N3–Ag1$^{(iv)}$ = 107.4(5), C5–N3–Ag1$^{(iv)}$ = 112.9(4); [Symmetry codes: (i) 1/2 + x,1/2–y,1–z; (ii) 1 + x,+y,+z; (iii) –1/2 + x,1/2–y,1–z; (iv) –1 + x,+y,+z].

coordinated **L** are almost identical, except that the *P*1-O11 distance (2.747(5) Å) in the coordination polymer is much longer than in the free **L** (2.661 Å).

Both oxygen atoms of the phosphabetaine carboxylate group and the N3 nitrogen of the phosphadamantane moiety coordinate to an Ag(I) located in a distorted tetrahedral coordination environment (Fig. 5), and as a result, a chain-polymer is formed.

The backbone of this two-dimensional polymer consists of a linear chain of alternating silver ions and carboxylate groups (Fig. 6).

The Ag1–N3$^{(i)}$ distance (2.288(6) Å) is one of the shortest known in Ag-PTA complexes; the shortest determined so far, 2.302 Å was found in the [Ag(μ-aba)(μ-PTA)]$_n$ × 3nH_2O (aba = aminobenzoate) complex [21]. The O3 atom of the triflate anion is also coordinated to the Ag(I)-ion, however, this interaction does not contribute to the formation of the chain-polymer (Fig. 7).

Weak C—H…F and C—H…O interactions also help to hold together the polymer chains, however, there are no significant second-order bonds (Fig. 7, Fig. S7C, Table S3).

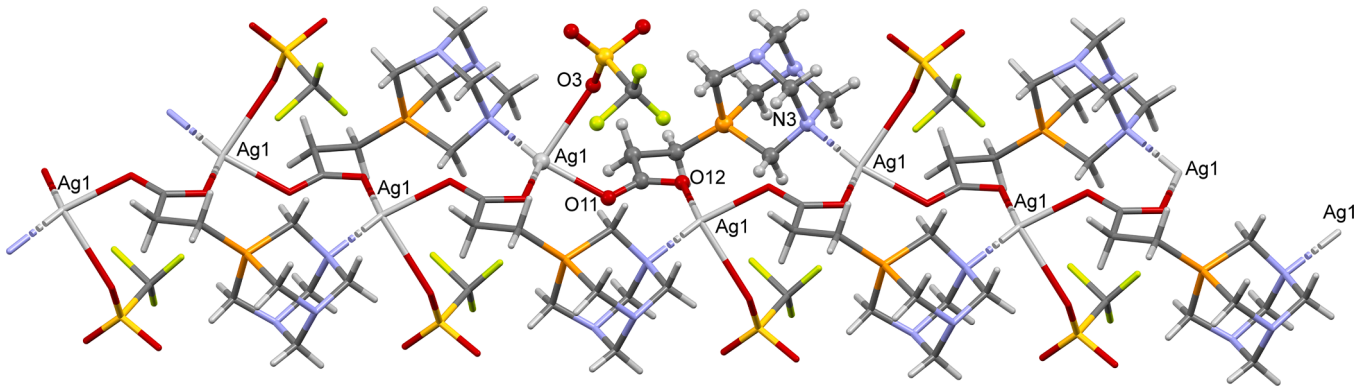

Fig. 7. Partial packing along axis "**c**" in ribbons of $[Ag(OTf)(\mu_3\text{-}\mathbf{L}\text{-}\kappa^3 N{:}O{:}O')]_n$, **3.** The asymmetric unit of **3** is given in ball and sticks, and the symmetry-generated part of the polymer is given in capped sticks representation.

Table 2
NMR spectral data for **L** and its silver(I)-based coordination polymers **1**–**3.**

	^{31}P NMR δ (ppm)	^{1}H NMR		
		δ (d, 6H, P^+–CH_2-N) (ppm)	δ (d, 3H, N-CH_2(eq)-N) (ppm)	δ (d, 3H, N-CH_2(ax)-N) (ppm)
L	–37.6	4.57 ($^2J_{P\text{-}H}$ = 6.6 Hz)	4.50 (J_{AB} = 13.2 Hz)	4.62 (J_{BA} = 13.6 Hz)
1	–37.5	4.60 ($^2J_{P\text{-}H}$ = 6.8 Hz)	4.53 (J_{AB} = 13.2 Hz)	4.65 (J_{BA} = 13.5 Hz)
2	–37.6	4.59 ($^2J_{P\text{-}H}$ = 6.8 Hz)	4.52 (J_{AB} = 13.2 Hz)	4.63 (J_{BA} = 13.6 Hz)
3	–37.6	4.60 ($^2J_{P\text{-}H}$ = 6.7 Hz)	4.53 (J_{AB} = 13.2 Hz)	4.65 (J_{BA} = 13.6 Hz)

*3.3. The molecular state of coordination polymers **1**–**3** in aqueous solutions*

In aqueous solutions, ^{31}P NMR spectra of the coordination polymers **1**–**3**, obtained in reactions of **L** and AgX-salts, show the characteristic singlet resonance of free **L** at δ = –37.6 ppm (Table 2). ^{1}H NMR spectra of the same solutions were also compared to the corresponding spectrum of **L** (Fig. 8). The resonances of the P^+–CH_2-CH_2-COO^- protons of free and coordinated **L** appear basically the same. However, there are small shifts in the P^+–CH_2-N and N-CH_2-N signals (Table 2, Fig. 8) indicating the coordination of Ag(I) to the nitrogen donor atoms of the ligand (see Fig. 9).

The most intense MS signals in the ESI-MS spectrum of $[Ag(\mu_3\text{-}\mathbf{L}\text{-}\kappa^3 N{:}O{:}O')]_n(PF_6)_n$ (**1**) recorded with the use of aqueous solutions are $[\mathbf{L} + Na]^+$, 252.0878 *m/z*, and $[2\mathbf{L} + Na]^+$, 481.1854 *m/z*. In the case of $[Ag(tos)(\mu_3\text{-}\mathbf{L}\text{-}\kappa^3 N{:}N{:}O)]_n{\cdot}nH_2O$ (**2**), the most intense peak also belongs to $[\mathbf{L} + Na]^+$, however the peaks belonging to $[\mathbf{L} + Ag]^+$ (336.0026 *m/z*) and $[2\mathbf{L} + Ag]^+$ (565.1009 *m/z*) could be detected, too. Finally, in the ESI-MS spectrum of $[Ag(OTf)(\mu_3\text{-}\mathbf{L}\text{-}\kappa^3 N{:}O{:}O')]_n$ (**3**), the most intense signals can be attributed to the $[\mathbf{L} + Ag]^+$ and $[2\mathbf{L} + Ag]^+$ Ag-containing fragments. Similar observations were published on the spectral characteristics of related PTA-Ag complexes [22–27]. For example, in the spectrum of $[Ag(\mu_2\text{-PTA}{:}\kappa^2 P{:}N)(\mu_2\text{-}O_2N{:}\kappa^2 O{:}O')]_n$ recorded with the use of methanol–water solvent mixture the main peak belonged to $[Ag(PTA)_2]^+$, and higher nuclearity species, such as $[Ag_2(PTA)_2(NO_2)]^+$ and

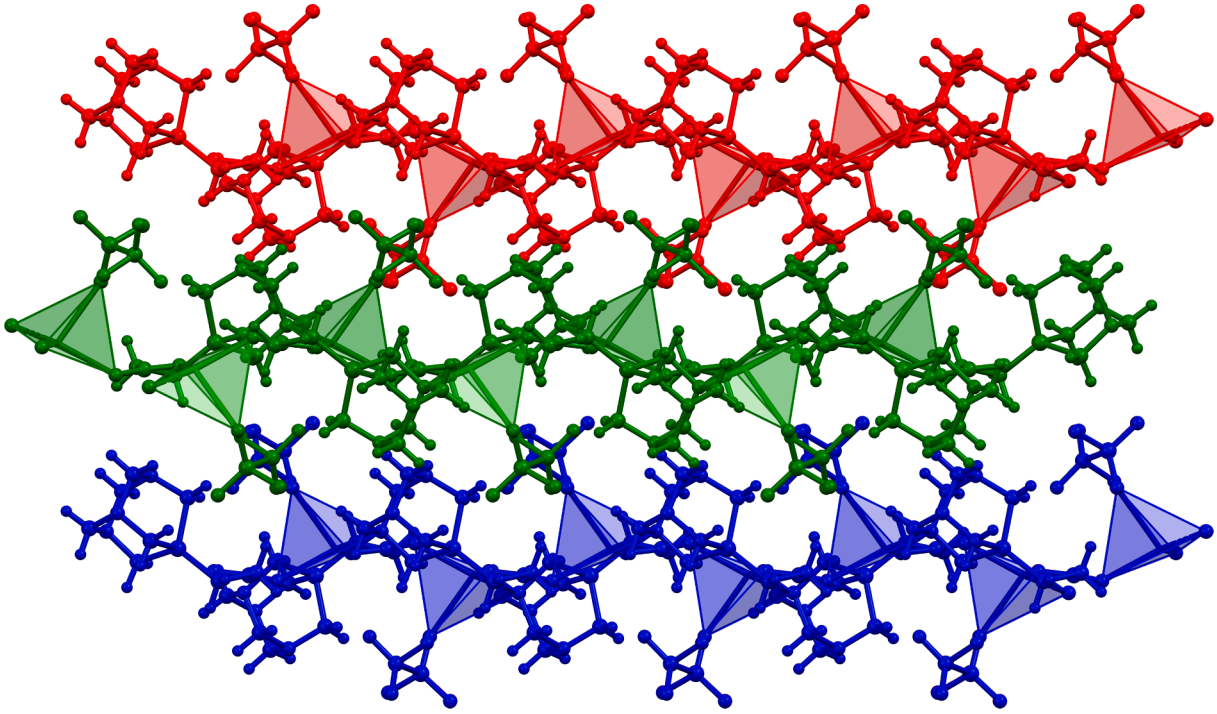

Fig. 8. Polymer chains with silver polyhedra in $[Ag(OTf)(\mu_3\text{-}\mathbf{L}\text{-}\kappa^3 N{:}O{:}O')]_n$, **3.** (Each chain is drawn in a different color.)

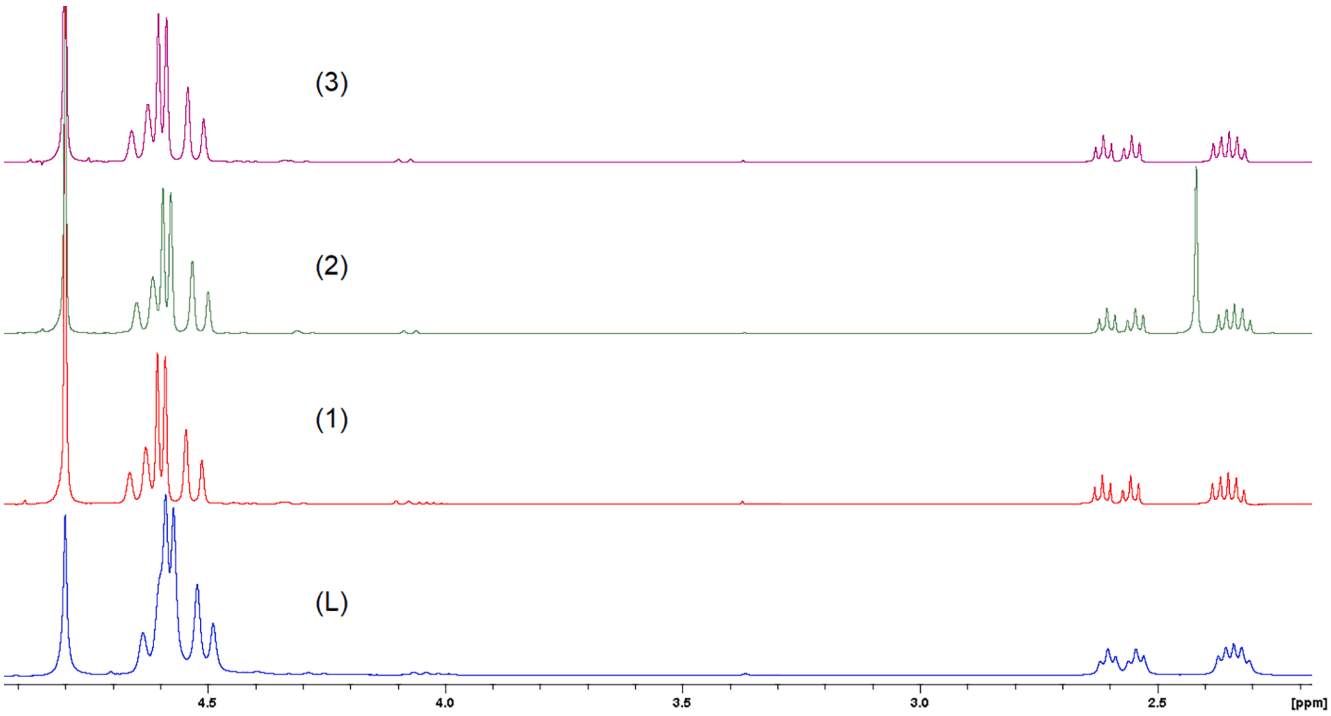

Fig. 9. Overlaid ^{1}H NMR spectra of aqueous solutions of **L, 1–3.**

$[Ag_2(PTA)_3(NO_2)]^+$ were detected only with low intensity [27].

The ESI-MS data could be rationalized by assuming that the mono- and dinuclear fragments were formed from the polymers during ionization. However, it seems probable, that already the interaction with the (aqueous) solvent leads to the break-up of the polymers into smaller units. To address this question, we carried out diffusion NMR measurements.

Diffusion NMR spectroscopy allows the determination of the diffusion coefficient of a diffusing ion, molecule or particle. The method is briefly outlined in *Section 2.1 Materials and methods*, and treated excellently in reviews and earlier papers [38–43] Diffusion coefficients can be used –with certain approximations and limitations– for calculation of the hydrodynamic diameters of the moving species according to the Einstein-Stokes relation. We reasoned that knowledge of the hydrodynamic parameters of **L** and **1–3** in aqueous solutions may help to reveal the molecular state of the species obtained upon dissolution of **1–3** in water. With this aim in mind, diffusion NMR experiments were performed with the use of the Pulsed Field Gradient Spin-Echo (PGSE) NMR method. According to the method, monodimensional NMR spectra were recorded as a function of varying pulsed-field gradient (G) in quadratic steps along the z axis.

Measurements involving **L** were performed on D_2O solutions with c_L = 0.044 M concentration at 298.0 ± 0.2 K. The ^{1}H NMR spectra displayed well-separated resonances of water and **L** (Fig. S8A, S8C). The integral values of the main peak of **L** and peak of water, as the function of the square of the pulsed-gradient field ($\gamma^2G^2\,\delta^2(\Delta-\delta/3)$), could be well fitted with a monoexponential function ($I = B \times e^{-G^2D}$) for both D_2O and **L** (Fig. S8B). From the data shown on Fig. S8B, the values of B were calculated as 17360.6 (D_2O) and 138,707 (**L**).

From these measurements, the diffusion coefficient of D_2O was calculated as $D = 1.62 \times 10^{-9}$ m^2 s^{-1}, which is lower than the value known from the literature (1.902×10^{-9} m^2 s^{-1} [44]). This difference may arise from the dynamics of water exchange between the hydration sphere of **L** and the bulk water phase. Namely, in the case of a fast exchange, the measurements yield an average diffusion coefficient of bulk and hydration sphere water molecules. For the diffusion coefficient of **L,** D = 5.22×10^{-10} m^2 s^{-1} was obtained. As mentioned before, calculations based on the Einstein–Stokes relation need approximations. In our approach, we regarded the solutions as infinitely dilute, so the actual viscosity of the solutions was taken equal to the viscosity of the solvent (water). Furthermore, the diffusing species were approximated spherical, moving randomly out from their given position. With these approximations, the hydrodynamic diameter of **L** was found d = 0.762 ± 0,002 nm (the uncertainty caused by the error of curve fitting).

Table 3
Diffusion coefficients and hydrodynamic diameters of **L** and compounds **1–3** in aqueous solution at T = 298.0 ± 0.2 K, determined by the PGSE NMR method.

	Diffusion coefficient (m^2 s^{-1})		Hydrodynamic diameter (nm)
	D_2O	Solute	Solute
L	1.62×10^{-9}	5.22×10^{-10}	0.762 ± 0.002
1	1.88×10^{-9}	5.53×10^{-10}	0.719 ± 0.001
2	1.89×10^{-9}	5.51×10^{-10}	0.722 ± 0.002
3	1.91×10^{-9}	5.57×10^{-10}	0.714 ± 0.001

With the same procedure as for **L**, diffusion coefficients and hydrodynamic diameters were also determined for compounds **1–3** in aqueous solutions. The data are shown in Table 3, the corresponding experimental results are shown on Figs. S9 – S11.

With regard to compound **2**, it is noted, that the 2D transformation of the ^{1}H NMR signals of the tosylate anion showed unequivocally an independent diffusion of tos and **L** (Fig. S10B). Diffusion coefficients were determined as 6.92×10^{-10} m^2 s^{-1} for tosylate, 5.51×10^{-10} m^2 s^{-1} for **L**, and 1.89×10^{-9} m^2 s^{-1} for D_2O, and the fitting error was smaller by two orders of magnitude (for tosylate) and by three orders of magnitude (for **L** and D_2O) than the fitted value.

Comparison of the values of the hydrodynamic diameters of **L** *vs* **1–3** in Table 3 leads to the conclusion, that coordination of the phosphabetaine **L** to Ag(I) results in shrinking of the total occupied space around the metal ion. Even with the approximations involved in the Einstein–Stokes equation, this result does not support the presence of high nuclearity species of coordination polymers **1–3** in aqueous solutions. Furthermore, dissolution of polymers usually leads to increased viscosity of the solutions related to the pure solvent, which results in slower

diffusion hence lower diffusion coefficient of the solvent. In contrast, in aqueous solutions of **1**–**3**, the diffusion coefficient of the solvent is close to that of the literature value of pure D_2O. This finding again supports the disaggregation of **1**–**3** in aqueous solutions. Taking these results together with the ESI–MS data discussed above, it may be concluded that in solution the supramolecular coordination effects and second order bonding are not sufficiently strong to maintain the polymeric structures determined unambiguously in the crystalline state of compounds **1**–**3**. These findings are in accord with the results of Kirillov and co-workers [24,26], who also came to the conclusion that related Ag–PTA–based coordination polymers disassembled in aqueous solutions and existed as oligomers, at most.

In summary, we have confirmed, that *P*-carboxyethyl-substituted derivatives of PTA may serve as new building blocks for novel self-assembling silver-organic networks. Depending on the nature of the anion of the Ag-salt used for building up the coordination polymers, significant differences can be obtained in the structure of the polymers as a result of the various possible N,N',O- or N,O,O'-coordination modes of the PTA-derived ligand. The obtained compounds extend a limited family of PTA-derived coordination polymers [7–9]. Furthermore, the high-yielding synthesis of **L** from acrylic acid and PTA in a ball-mill is in striking contrast to the unsuccessful attempts to obtain **L** in solution from the same reactants and demonstrates the effectiveness of mechanochemical synthesis.

Funding

The research was supported by the EU and co-financed by the European Regional Development Fund (under the projects GINOP-2.3.2-15-2016-00008 and GINOP-2.3.3-15-2016-00004), and by the Thematic Excellence Programme of the Ministry for Innovation and Technology of Hungary (ED_18-1-2019-0028), within the framework of the Vehicle Industry thematic programme of the University of Debrecen. The financial support of the Hungarian National Research, Development and Innovation Office (FK-128333) is greatly acknowledged.

CRediT authorship contribution statement

Antal Udvardy: Conceptualization, Investigation, Writing - original draft, Writing - review & editing. **Csenge Tamara Szolnoki:** Investigation. **Éva Kováts:** Investigation, Writing - original draft, Writing - review & editing. **Dávid Nyul:** Methodology, Investigation, Writing - original draft. **Gyula Tamás Gál:** Methodology, Investigation. **Gábor Papp:** Methodology, Writing - review & editing. **Ferenc Joó:** Writing - original draft, Writing - review & editing, Resources. **Ágnes Kathó:** Conceptualization, Writing - original draft, Writing - review & editing, Supervision.

Declaration of Competing Interest

The authors declare that they have no known competing financial interests or personal relationships that could have appeared to influence the work reported in this paper.

Acknowledgement

The authors are grateful to Dr. Attila C. Bényei for recording the X-ray diffraction data. Thanks are expressed to Ms. Cynthia Nagy for the HR ESI-MS measurements.

Appendix A. Supplementary data

Supplementary data to this article can be found online at https://doi.org/10.1016/j.ica.2021.120299.

References

[1] H. Vardhan, M. Yusubov, F. Verpoort, Self-assembled metal–organic polyhedra: An overview of various applications, Coord. Chem. Rev. 306 (2016) 171–194, https://doi.org/10.1016/j.ccr.2015.05.016.
[2] C. Wang, X. Liu, N. Keser Demir, J.P. Chen, K. Li, Applications of water stable metal–organic frameworks, Chem. Soc. Rev. 45 (18) (2016) 5107–5134, https://doi.org/10.1039/C6CS00362A.
[3] F. Beuerle, B. Gole, Covalent organic frameworks and cage compounds: design and applications of polymeric and discrete organic scaffolds, Angew. Chem. Int. Ed. 57 (18) (2018) 4850–4878, https://doi.org/10.1002/anie.201710190.
[4] N. Gimeno, R. Vilar, Anions as templates in coordination and supramolecular chemistry, Coord. Chem. Rev. 250 (23-24) (2006) 3161–3189, https://doi.org/10.1016/j.ccr.2006.05.016.
[5] A.K. Gupta, D.M. Salazar, A. Orthaber, Solvent and counter-ion induced coordination environment changes towards Ag^{I} coordination polymers, Eur. J. Inorg. Chem. 2019 (33) (2019) 3740–3744, https://doi.org/10.1002/ejic.201900722.
[6] H. He, L. Hashemi, M.-L. Hu, A. Morsali, The role of the counter-ion in metal-organic frameworks' chemistry and applications, Coord. Chem. Rev. 376 (2018) 319–347, https://doi.org/10.1016/j.ccr.2018.08.014.
[7] A.D. Phillips, L. Gonsalvi, A. Romerosa, F. Vizza, M. Peruzzini, Coordination chemistry of 1,3,5-triaza-7-phosphaadamantane (PTA): Transition metal complexes and related catalytic, medicinal and photoluminescent applications, Coord. Chem. Rev. 248 (11-12) (2004) 955–993, https://doi.org/10.1016/j.ccr.2004.03.010.
[8] J. Bravo, S. Bolaño, L. Gonsalvi, M. Peruzzini, Coordination chemistry of 1,3,5-triaza-7- phosphaadamantane (PTA) and derivatives. Part II. The quest for tailored ligands, complexes and related applications, Coord. Chem. Rev. 254 (5-6) (2010) 555–607, https://doi.org/10.1016/j.ccr.2009.08.006.
[9] A. Guerriero, M. Peruzzini, L. Gonsalvi, Coordination chemistry of 1,3,5-triaza-7-phosphatricyclo[3.3.1.1]decane (PTA) and derivatives. Part III. Variations on a theme: Novel architectures, materials and applications, Coord. Chem. Rev. 355 (2018) 328–361, https://doi.org/10.1016/j.ccr.2017.09.024.
[10] C. Lidrissi, A. Romerosa, M. Saoud, M. Serrano-Ruiz, L. Gonsalvi, M. Peruzzini, Stable, water-soluble PTA-based Ru–Ag organometallic polymers, Angew. Chem. 117 (17) (2005) 2624–2628, https://doi.org/10.1002/ange.200462790.
[11] M. Serrano Ruiz, A. Romerosa, B. Sierra-Martin, A. Fernandez-Barbero, A water soluble diruthenium–gold organometallic microgel, Angew. Chem. Int. Ed. 47 (45) (2008) 8665–8669, https://doi.org/10.1002/anie.200803232.
[12] M. Serrano-Ruiz, S. Imberti, L. Bernasconi, N. Jadagayeva, F. Scalambra, A. Romerosa, Study of the interaction of water with the aqua-soluble dimeric complex $[RuCp(PTA)_2\text{–}\mu\text{-}CN\text{–}1\kappa C{:}2\kappa^2N\text{-}RuCp(PTA)_2](CF_3SO_3)$ (PTA = 1,3,5-triaza-7-phosphaadamantane) by neutron and X-ray diffraction in solution, Chem. Commun. 50 (78) (2014) 11587–11590, https://doi.org/10.1039/C4CC05225K.
[13] M. Serrano Ruiz, F. Scalambra, A. Romerosa, First water-soluble backbone Ru–Ru–Ni heterometallic organometallic polymer, Macromol. Rapid Commun. 36 (2015) 689–693, https://doi.org/10.1002/marc.201400657.
[14] F. Scalambra, M. Serrano-Ruiz, D. Gudat, A. Romerosa, Amorphization of a Ru-Ru-Cd-coordination polymer at low pressure, ChemistrySelect 1 (5) (2016) 901–905, https://doi.org/10.1002/slct.201600242.
[15] B. Sierra-Martin, M. Serrano-Ruiz, V. García-Sakai, F. Scalambra, A. Romerosa, A. Fernandez-Barbero, Self-organization and swelling of ruthenium-metal coordination polymers with PTA (metal = Ag, Au, Co), Polymers 10 (2018) 528, https://doi.org/10.3390/polym10050528.
[16] F. Scalambra, M. Serrano-Ruiz, A. Romerosa, Water driven formation of channels: unusual solid-state structural transformation of a heterometallic polymer, Dalton Trans. 47 (10) (2018) 3588–3595, https://doi.org/10.1039/C7DT04515H.
[17] F. Scalambra, S. Rudić, A. Romerosa, Molecular insights into bulk and porous κ^2P, N-PTA metal organic polymers by simultaneous raman spectroscopy and inelastic neutron scattering, Eur. J. Inorg. Chem. (2019) 1155–1161, https://doi.org/10.1002/ejic.201801283.
[18] B. Sierra-Martin, M. Serrano Ruiz, F. Scalambra, A. Fernandez-Barbero, A. Romerosa, Novel ruthenium-silver PTA-based polymers and their behavior in water, Polymers 11 (2019) 1249, https://doi.org/10.3390/polym11081249.
[19] F. Scalambra, B. Sierra-Martin, M. Serrano-Ruiz, A. Fernandez-Barbero, A. Romerosa, First exfoliated Ru–Ru–Au organometallic polymer with layered structure, Chem. Commun. 56 (66) (2020) 9441–9444, https://doi.org/10.1039/D0CC04325G.
[20] F. Mohr, L.R. Falvello, M. Laguna, A Silver(I),, coordination polymer containing tridentate N- and P-coordinating 1,3,5-triaza-7-phosphaadamantane (PTA) ligands, Eur. J. Inorg. Chem. (2006) 3152–3154, https://doi.org/10.1002/ejic.200600455.
[21] A. Lis, M.F.C.G. da Silva, A.M. Kirillov, P. Smolenski, A.J.L. Pombeiro, Design of Silver(I)-PTA coordination polymers through controlled N, P-coordination of 1,3,5-triaza-7-phosphaadamantane (PTA) with arylcarboxylates, Cryst. Growth Des. 10 (12) (2010) 5244–5253, https://doi.org/10.1021/cg101058x.
[22] A.M. Kirillov, S.W. Wieczorek, M.F.C. Guedes da Silva, J. Sokolnicki, P. Smolenski, A.J.L. Pombeiro, Crystal engineering with 1,3,5-triaza-7-phosphaadamantane (PTA): first PTA-driven 3D metal–organic frameworks, CrystEngComm 13 (2011) 6329–6333, https://doi.org/10.1039/C1CE05612C.
[23] P. Smolenski, S.W. Jaros, C. Pettinari, G. Lupidi, L. Quassinti, M. Bramucci, L. A. Vitali, D. Petrelli, A. Kochel, A.M. Kirillov, New water-soluble polypyridine silver(I) derivatives of 1,3,5-triaza-7-phosphaadamantane (PTA) with significant antimicrobial and antiproliferative activities, Dalton Trans. 42 (2013) 6572–6581, https://doi.org/10.1039/C3DT33026E.

[24] S.W. Jaros, M.F.C. Guedes da Silva, M. Florek, M.C. Oliveira, P. Smoleński, A.J. L. Pombeiro, A.M. Kirillov, Aliphatic dicarboxylate directed assembly of silver(I) 1,3,5-triaza-7-phosphaadamantane coordination networks: topological versatility and antimicrobial activity, Cryst. Growth Des. 14 (11) (2014) 5408–5417, https://doi.org/10.1021/cg500557r.
[25] S.W. Jaros, M.F.C. Guedes da Silva, J. Król, M.C. Oliveira, P. Smoleński, A.J. L. Pombeiro, A.M. Kirillov, Bioactive silver–organic networks assembled from 1,3,5-triaza-7-phosphaadamantane and flexible cyclohexanecarboxylate blocks, Inorg. Chem. 55 (4) (2016) 1486–1496, https://doi.org/10.1021/acs.inorgchem.5b02235.
[26] S.W. Jaros, M.F.C. Guedes da Silva, M. Florek, P. Smolenski, A.J.L. Pombeiro, A. M. Kirillov, Silver(I) 1,3,5-triaza-7-phosphaadamantane coordination polymers driven by substituted glutarate and malonate building blocks: self-assembly synthesis, structural features, and antimicrobial properties, Inorg. Chem. 55 (12) (2016) 5886–5894, https://doi.org/10.1021/acs.inorgchem.6b00186.
[27] S.W. Jaros, M. Haukka, M. Florek, M.F.C. Guedes da Silva, A.J.L. Pombeiro, A. M. Kirillov, P. Smolenski, New microbe killers: Self-assembled silver(I) coordination polymers driven by a cagelike aminophosphine, Materials 12 (2019) 3353–3363, https://doi.org/10.3390/ma12203353.
[28] S.W. Jaros, J. Król, B. Bazanów, D. Poradowski, A. Chrószcz, D.S. Nesterov, A. M. Kirillov, P. Smoleński, Antiviral, antibacterial, antifungal, and cytotoxic silver (I) bioMOF assembled from 1,3,5-triaza-7-phoshaadamantane and pyromellitic acid, Molecules 25 (2020) 2119, https://doi.org/10.3390/molecules25092119.
[29] Sizwe J. Zamisa, Bernard Omondi, Synthesis and structural elucidation of 1-D silver(I) aliphatic carboxylate coordination polymers with 1,3,5-triaza-7-phosphaadamantane/N-methyl-1,3,5-triaza-7-phosphaadamantane, J. Coord. Chem. 69 (20) (2016) 3043–3052, https://doi.org/10.1080/00958972.2016.1227801.
[30] L. Jaremko, A.M. Kirillov, P. Smoleński, A.J.L. Pombeiro, Engineering Coordination and Supramolecular Copper-Organic Networks by Aqueous Medium Self-Assembly with 1,3,5-Triaza-7-phosphaadamantane (PTA), Cryst. Growth Des. 9 (2009) 3006–3010, doi: 10.1021/cg900334w.
[31] A.M. Kirillov, S.W. Wieczorek, A. Lis, M.F.C. Guedes da Silva, M. Florek, J. Krol, Z. Staroniewicz, P. Smolenski, A.J.L. Pombeiro, 1,3,5-Triaza-7-phosphaadamantane-7-oxide (PTA=O): new diamondoid building block for design of three-dimensional metal-organic frameworks, Cryst. Growth Des. 11 (2011) 2711–2716, https://doi.org/10.1039/C3CE40913A.
[32] S.W. Jaros, P. Smoleński, M.F.C. Guedes da Silva, M. Florek, J. Król, Z. Staroniewicz, A.J.L. Pombeiro, A.M. Kirillov, New silver BioMOFs driven by 1,3,5-triaza-7-phosphaadamantane-7-sulfide (PTA=S): synthesis, topological analysis and antimicrobial activity, CrystEngComm 15 (2013) 8060–8064, https://doi.org/10.1039/C3CE40913A.
[33] S.W. Jaros, U. Sliwinska-Hill, A. Bialonska, D.S. Nesterov, P. Kuropka, J. Sokolnicki, B. Bazanow, P. Smolenski, Light-stable polypyridine silver(i) complexes of 1,3,5-triaza-7-phosphaadamantane (PTA) and 1,3,5-triaza-7-phosphaadamantane-7-sulfide (PTAS): significant antiproliferative activity of representative examples in aqeueous media, Dalton Trans. 48 (2019) 11235–11249, https://doi.org/10.1039/C9DT01646E.
[34] S.W. Jaros, J. Sokolnicki, A. Wołoszyn, M. Haukka, A.M. Kirillov, P. Smoleński, Novel 2D coordination network built from hexacopper(I)-iodide clusters and cagelike aminophosphine blocks for reversible “turn on” sensing of aniline, J. Mater. Chem. C 6 (2018) 1670–1678, https://doi.org/10.1039/C7TC03863A.
[35] Z. He, X. Tang, Y. Chen, Z. Hea, The first air-stable and efficient nucleophilic trialkylphosphine organocatalyst for the Baylis-Hillman reaction, Adv. Synth. Catal. 348 (4-5) (2006) 413–417, https://doi.org/10.1002/adsc.200505403.
[36] X. Tang, B. Zhang, Z. He, R. Gao, Z. Hea, 1,3,5-Triaza-7-phosphaadamantane (PTA): A practical and versatile nucleophilic phosphine organocatalyst, Adv. Synth. Catal. 349 (11-12) (2007) 2007–2017, https://doi.org/10.1002/adsc.200700071.
[37] D.J. Daigle, A.B. Pepperman, S.L. Vail, Synthesis of a monophosphorus analog of hexamethylenetetramine, J. Heterocyclic Chem. 11 (1974) 407–408, doi: 10.1002/jhet.5570110326.
[38] R. Kimmich, NMR-Tomography, Diffusometry, Relaxometry, Springer, Berlin, 1998.
[39] I. Ardelean, R. Kimmich, Principles and unconventional aspects of NMR diffusometry, in Annual Reports on NMR Spectroscopy 49 (2003) 43–115. Elsevier, doi: 10.1016/S0066-4103(03)49002-9.
[40] A. Macchioni, G. Ciancaleoni, C. Zuccaccia, D. Zuccaccia, Determining accurate molecular sizes in solution through NMR diffusion spectroscopy, Chem. Soc. Rev. 37 (3) (2008) 479–489, https://doi.org/10.1039/B615067P.
[41] S. Bolaño, G. Ciancaleoni, J. Bravo, L. Gonsalvi, A. Macchioni, M. Peruzzini, PGSE NMR studies on RAPTA derivatives: evidence for the formation of H-Bonded dicationic Species, Organometallics 27 (7) (2008) 1649–1652, https://doi.org/10.1021/om701131s.
[42] I. Bányai, M. Kéri, Z. Nagy, M. Berka, L.P. Balogh, Self-diffusion of water and poly (amidoamine) dendrimers in dilute aqueous solutions, Soft Matter 9 (5) (2013) 1645–1655, https://doi.org/10.1039/C2SM26726H.
[43] M. Kéri, C. Peng, X. Shi, I. Bányai, NMR characterization of PAMAM_G5.NH_2 entrapped atomic and molecular assemblies, J. Phys. Chem. B 119 119 (7) (2015) 3312–3319.
[44] R. Mills, Self-diffusion in normal and heavy water in the range 1–45°, J. Phys. Chem. 77 (1973) 685–688, https://doi.org/10.1021/j100624a0.
[45] B. V. Nonius, CAD-Express Software, Ver. 5.1/1.2. Enraf Nonius, Delft, The Netherlands. 1994.; K. Harms, S. Wocaldo, XCAD4, University of Marburg, Germany, 1995.
[46] Rigaku (2015). CrysAlisPro Software System, Version 1.171.38.41. Rigaku Oxford Diffraction, http://www.rigaku.com.
[47] G.M. Sheldrick, SHELXT—Integrated space-group and crystal-structure determination, Acta Cryst. A 71 (2015) 3–8, https://doi.org/10.1107/S2053273314026370.
[48] G.M. Sheldrick, Crystal structure refinement with SHELXL, Acta Cryst. C 71 (2015) 3–8, https://doi.org/10.1107/S2053229614024218.
[49] O.V. Dolomanov, L.J. Bourhis, R.J. Gildea, A.J.K. Howard, H. Puschmann, $OLEX^2$: A complete structure solution, refinement and analysis program, J. Appl. Cryst. 42 (2009) 339–341, https://doi.org/10.1107/S0021889808042726.
[50] L.J. Farrugia, WinGX and ORTEP for Windows: an update, J. Appl. Cryst. 45 (2012) 849–854, https://doi.org/10.1107/S0021889812029111.
[51] A.L. Spek, checkCIF validation ALERTS: what they mean and how to respond, Acta Cryst. E 76 (2020) 1–11, https://doi.org/10.1107/S2056989019016244.
[52] C.F. Macrae, I.J. Bruno, J.A. Chisholm, P.R. Edgington, P. McCabe, E. Pidcock, L. Rodriguez-Monge, R. Taylor, J.V.D. Streek, P.A. Wood, Mercury CSD 2.0—New features for the visualization and investigation of crystal structures, J. Appl. Cryst. 41 (2008) 466–470, https://doi.org/10.1107/S0021889807067908.
[53] A. Udvardy, M. Purgel, T. Szarvas, F. Joó, Á. Kathó, Synthesis and structure of stable water-soluble phosphonium alkanoate zwitterions derived from 1,3,5-triaza-7-phosphaadamantane, Struct. Chem. 26 (2015) 1323–1334, https://doi.org/10.1007/s11224-015-0618-4.
[54] The Cambridge Structural Database. C.R. Groom, I. J. Bruno, M.P. Lightfoot, S.C. Ward, Acta Cryst. B72 (2016) 171–179, doi: 10.1107/S2052520616003954. (CSD, 5.41, 2020, May.).
[55] H. Wu, M.-X. Shang, S.-P. ShangGuana, Poly[[aquatris-(μ_3-hexamethylenetetramine-κ^3 *N, N′, N″*)tris(p-toluenesulfonato-κO)trisilver(I)] trihydrate], Acta Cryst. E 66 (2010) m1665–m1666, https://doi.org/10.1107/S1600536810048567.